ISSN 1993-9973, e-ISSN 2415-332X

Vol. 26, No. 1
2026

PROSPECTING AND DEVELOPMENT OF OIL AND GAS FIELDS

https://pdogf.com.ua/en

Received: 20.11.2025. Revised: 01.05.2026. Accepted: 29.05.2026. Published: 29.06.2026.

UDC 621.793:539.538

DOI: 10.63341/pdogf/1.2026.41

# Microstructural evolution and wear resistance of Ti-based MAX phases doped with X-elements for use in drilling and hydrocarbon production

**Marine Sasuntsyan***

PhD in Technical Sciences, Associate Professor
National Polytechnic University of Armenia
0009, 105 Teryan Str., Yerevan, Armenia
https://orcid.org/0009-0000-6769-114X

**Nina Sahakyan**

PhD in Technical Sciences
National Polytechnic University of Armenia
0009, 105 Teryan Str., Yerevan, Armenia
https://orcid.org/0009-0007-6511-7129

**Serob Hayrapetyan**

PhD in Technical Sciences, Researcher
National Polytechnic University of Armenia
0009, 105 Teryan Str., Yerevan, Armenia
https://orcid.org/0009-0008-4576-2371

**Suren Aghbalyan**

Postgraduate Student
National Polytechnic University of Armenia
0009, 105 Teryan Str., Yerevan, Armenia
https://orcid.org/0000-0001-9987-8515

**Abstract.** The purpose of the study was to establish how doping with various X elements affects the microstructural evolution of Ti-based MAX-phase alloys and how these changes affect hardness, thermophysical and tribological properties. The methodology provided for obtaining the base and doped series of Ti-Al-C alloys and their study by X-ray phase analysis, scanning electron microscopy, energy dispersion analysis, digital morphometry, microindentation, resonance determination of elastic modulus, dilatometry, thermogravimetric analysis, tribological tests, and statistical data processing. As a result, it was found that the base series retains the dominance of $Ti_3AlC_2$ at 87% and is characterised by the most ordered lamellar microstructure with an average grain size of 8.3 μm. Iron doping reduces the proportion of $Ti_3AlC_2$ to 62%, increases the TiC content to 28%, and is accompanied by the appearance of $Fe_3Al$, grain grinding to 5.7 μm, violation of the lamellar architecture, and the development of a heterogeneous carbide-intermetallic ensemble. This provides a maximum microhardness of 5.1 GPa, but simultaneously leads to a decrease in the elastic modulus to 191 GPa, density to 4.17 g/cm$^3$, electrical conductivity to $2.1 \times 10^4$ S/m, an increase in the coefficient of linear thermal expansion to 9.7 × 10-6 1/°C, mass loss according to the results of thermogravimetric analysis to 8.6%, and the worst tribological indicators. Silicon doping preserves $Ti_3AlC_2$ at 74%, is accompanied by the formation of $Ti^5Si_3$, supports a more ordered intergranular organisation with an average grain size of 6.9 μm and forms the most balanced complex of properties: microhardness 4.2 GPa, modulus of elasticity 214 GPa, density 4.44 g/cm$^3$, electrical conductivity $3.2 \times 10^4$ S/m, coefficient

**Suggested Citation:** Sasuntsyan, M., Sahakyan, N., Hayrapetyan, S., Aghbalyan, S. (2026). Microstructural evolution and wear resistance of Ti-based MAX phases doped with X-elements for use in drilling and hydrocarbon production. *Prospecting and Development of Oil and Gas Fields*, 26(1), 41-55. doi: 10.63341/pdogf/1.2026.41.

*Corresponding author (*sasuntsyanmarine@gmail.com*)

of linear thermal expansion $7.5 \times 10^{-6}$ 1/°C, mass loss according to the results of thermogravimetric analysis – 3.4%, mass loss at friction – 3.4%, wear – 0.28 C.U., and the coefficient of friction – 0.47. The practical significance of the results lies in the possibility of their use in the development and selection of wear-resistant Ti-based MAX materials and coatings for drilling and oil and gas production equipment

**Keywords:** carbide development; tribological behaviour; grain size; modulus of elasticity; thermal conductivity; hardness

## Introduction

Ti-based MAX-phases-layered carbides or carbonitrides of transition metals with the general formula $M_{n+1}AX_n$, doped with X-elements, attract increasing attention in materials science and engineering as a class of materials in which the layered crystal structure is combined with high chemical and thermal stability, satisfactory mechanical characteristics, and the ability to work under difficult contact load conditions. Interest in such systems increases in those applications where the material must simultaneously withstand abrasive effects, friction heating, cyclic stress changes, and long-term operation in an aggressive environment. These conditions include the processes of drilling and extraction of hydrocarbons, in which the durability of structural elements and coatings is determined not by a separate parameter, but by a set of interrelated characteristics. In this mode of operation, the analysis covers the stability of lamellar morphology, the state of grain boundaries, the distribution of secondary phases, hardness, thermal conductivity, and the nature of wear under external loads. Therefore, doping with X elements should not be considered as a local compositional change, but as a factor capable of rearranging the phase equilibrium, microstructural organisation, and functional behaviour of Ti-based MAX phases.

An important foundation for this understanding was laid by N.N. Aghajanyan *et al*. (2023), who investigated the self-propagating high-temperature synthesis of MAX phases in the Ti-Zr-Al-C system. The paper showed that variations in the composition of the initial mixture and synthesis conditions directly affect the phase composition, lattice parameters, and microstructure features, and therefore, composite control is one of the basic mechanisms for controlling structure formation. Further disclosure of this approach was contained in the paper by G.N. Muradyan (2023), where Ti-Al-C-based MAX phases were considered in the framework of synthesis in the hydride cycle. The study clearly linked the phase state of the material with the conditions of development and the course of reaction processes, which is why the technological route was not a background circumstance, but an active factor in the development of the final structure. A broader generalising view was suggested by S. Aydinyan (2023), who analysed the synthesis of MAX phases by combustion and emphasised that the microstructure and properties of such materials are determined by the production method itself. As a result, the lamellar organisation, the level of defects, and the presence of side phases appear as a natural result of a particular technological scheme, and not as random accompanying phenomena. A significant contribution to understanding the role of substitution in Ti-based MAX systems was made by M. Berrabah *et al*. (2025), who synthesised and characterised a new solid solution . Combining microstructural analysis with the study of transport properties showed that NB doping affects not only phase stability, but also functional parameters of the material.

A similar content vector result was obtained by M. Shahbaz *et al*. (2024) during the study of chromium-aluminium carbide MAX phases. The paper confirmed that a change in the chemical composition can lead to the development of structurally different MAX-like phases, so the choice of a doping element takes on the significance of a directional phase design tool. The functional measurement of TI-containing carbide systems was further revealed in the paper by B. Liu *et al*. (2026), where the Ti-C composite interlayer formed in situ was associated with increased corrosion resistance and electrical conductivity. This formulation of the question shifted attention to the role of microstructural architecture in the organisation of conducting pathways and once again emphasised that transport characteristics in multiphase Ti-based systems are structurally determined. A direct approach to tribological problems was traced in the study by H. Wu *et al*. (2025), devoted to the effect of Nb content on the properties of laser-deposited Ti-Al-CMAX-phase composite coatings. The results showed that the change in the doping component is accompanied by a simultaneous rearrangement of the phase ensemble, microstructure, and friction behaviour, and this indicates a complex nature of wear resistance development. This line was supported by Y. Lu *et al*. (2024), who investigated CoNi coatings reinforced with $Ti_2AlC$ and $Ti_3AlC_2$, using analyses of nanostructure, tribological properties, and density functional theory calculations. The study showed that the presence of the MAX-phase component is associated with an improvement in the tribological response, while interfacial interaction and the nature of structural organisation affect the mechanisms of wear. The influence of technological parameters on the development of the durability of Ti-Al-C systems was traced in detail by H. Hong *et al*. (2025). The researchers proved that the powder composition and processing parameters significantly change the microstructure and tribological behaviour of coatings, therefore, wear resistance was formed as a result of the joint action of the composition and technology. A related aspect of functional tribological optimisation was presented in the study by X. Gui *et al*. (2025) on Cu-$Ti_2AlC$ coatings. The paper showed that the High-Velocity Oxy-Fuel spraying parameters affect the wear mechanisms and efficiency of the MAX-phase component, which once again

emphasises the multi-factor nature of the behaviour of MAX-phase systems in friction mode.

The totality of these studies has shown that ideas about phase formation, microstructural development, transport characteristics, and tribological behaviour of Ti-based MAX systems have already acquired sufficient depth, but these lines of analysis are mostly deployed not in a single research field, but in partially separate areas. As a result, the complete scheme of interpretation of Ti-Al-X MAX phases, within which microstructural evolution, hardness, thermal conductivity and wear resistance would be considered as interrelated consequences of doping with various X elements, remains insufficiently developed. In many studies, the phase composition and features of synthesis are described without a sufficiently detailed tribological interpretation, whereas in studies focused on wear, the behaviour of the material is not always associated with the evolution of lamellar morphology, the state of grain boundaries, and the redistribution of secondary phases. This is what makes it necessary to study where the effect of X elements in Ti-based MAX phases will be analysed through the relationship between structure, hardness, and wear resistance under conditions typical of drilling and hydrocarbon production. The purpose of the study was to establish the features of the influence of various X-elements on the microstructural evolution of Ti-based MAX-phase alloys and related changes in hardness, thermophysical, and tribological properties.

## Materials and Methods

The study was conducted during 2025 at the Basic Research Laboratory of Materials Science and Metallurgy at the National Polytechnic University of Armenia (Yerevan). It was of a comparative nature and covered three series of Ti-based MAX alloys in the Ti-Al-C system: base without doping, Fe-doped and Si-doped. This design allowed comparing the effect of the type of doping element on the phase composition, microstructure, mechanical, thermophysical and tribological characteristics of the material under the same synthesis conditions. Dispersed powders of titanium (Ti, 99.5%, <45 μm, Alfa Aesar, USA), aluminium (Al, 99.9%, <50 μm, Sigma-Aldrich, Germany), carbon in the form of graphite (99.9%, <20 μm, Merck, Germany), and powder doping additives Fe and Si of high purity (Alfa Aesar, USA) were used as starting components. At the stage of model study of compositions, Fe and Si were considered as X-elements, which differ in the nature of interaction with the Ti-Al-C matrix, the ability to form secondary phases, and the effect on the stability of the lamellar structure. The base series without doping was used as a reference, and the doped series was formed under comparable synthesis conditions, which helped to correctly link the detected differences with the action of the doping factor.

Before mixing, the powder components were dried at 100°C for 24 hours. The charge was prepared in a Retsch PM100 planetary ball mill (Germany) at 300 rpm for 6 hours in an argon atmosphere using steel balls with a mass ratio of balls to powder of 10:1. This regime ensured sufficient uniformity in the distribution of components and reduced the risk of local segregation. After mixing, the powder compositions were compacted by cold isostatic pressing into cylindrical samples with a diameter of 20 mm at a pressure of 200 MPa on an AIP KIP-100 installation (Japan). Further development of the dense structure and the course of phase formation were provided by vacuum sintering in the Carbolite Gero STF 15/610 (UK) furnace at a temperature of 1,350°C with an exposure time of 2 hours and a heating rate of 10°C/min, after which the furnace was cooled to room temperature. To obtain representative results, three series of samples were prepared that differed in the type of doping element: basic without doping, Fe-doped and Si-doped, under the same pressing and sintering conditions. The phase composition of the synthesised materials was determined by X-ray diffraction on a Bruker D8 Advance diffractometer (Germany) using CuKα- radiation ($\lambda = 1.5406$ Å) in the range $2\theta$ from 20° to 80°, with a step of 0.02° and an accumulation time of 1 s per point. Phase identification was performed using a PDF-4+ database, and primary diffraction processing, reflex comparison, and phase composition refinement were performed in HighScore Plus. This approach allowed recording the main MAX phase, carbide and intermetallic components, and to assess trends towards stabilisation or destabilisation of the layered structure depending on the nature of the doping element.

Microstructural analysis was performed using a Tescan VEGA3 scanning electron microscope (Czech Republic) equipped with an energy-dispersive X-ray analyser Oxford Instruments X-MAX (United Kingdom). Polished cross-sections and fractographic surfaces were investigated, which allowed assessing the nature of morphology, spatial phase distribution, localisation of secondary inclusions, the state of interfacial boundaries, and signs of structural destabilisation. Energy dispersion analysis was used to clarify the local chemical composition of individual zones. The average grain size was determined by linear cross-section using scanning electron microscopy images. For this purpose, digital morphometry of scanning electron microscopy (SEM images) was performed in the Fiji software environment, followed by statistical processing of the measured values for each series of samples. This allowed moving from descriptive analysis of the microstructure to quantitative comparison of the degree of its rearrangement in different series of samples. The mechanical unit of the study included measurements of microhardness and elastic modulus. Microhardness was determined on a Buehler Micromet 5101 device (USA) at a load of 50 g; for each series, 10 measurements were performed in different sections of the section, which allowed considering the local inhomogeneity of the structure. The elastic modulus was evaluated by the resonant method on the IMCE RFDA system (Belgium) at longitudinal and transverse resonant frequencies. The density of the samples was determined by the Archimedes method, which allowed linking mechanical parameters with the degree of compaction, porosity, and features of the phase composition.

Functional characteristics included determination of electrical conductivity, coefficient of linear thermal expansion, and oxidative heat resistance. Electrical conductivity was measured by the four-probe method on a Loresta GP MCP-T610 instrument (Japan). The coefficient of linear thermal expansion was determined on a Linseis L75 PT dilatometer (Germany) in the temperature range from 25°C to 800°C. Oxidative heat resistance was analysed by thermogravimetric analysis on a Jupiter Netzsch STA 449 F3 (Germany) in an air atmosphere heated to 1,000°C at a rate of 10 °C/min with continuous recording of mass changes. This allowed comparing the functional parameters with the phase composition, the state of grain boundaries, and the distribution of secondary phases.

To assess wear resistance, tribological tests were carried out under dry friction conditions using the ball-on-disk method, with a 6 mm diameter AISI 52100 steel counter-body. The tests were performed at a normal load of 5 N, a sliding speed of 0.1 m/s, and a total friction path of 300 m at room temperature. At least three repetitions were performed for each series of samples. During the tests, the coefficient of friction was recorded, and after the test was completed, the mass loss and the amount of wear were determined. Thus, wear resistance was interpreted as an integral manifestation of the phase composition, microstructure, hardness, density, and functional stability of the material under tribological interaction conditions.

The methodological scheme of the study was based on a sequential combination of phase, microstructural, mechanical, thermophysical, and tribological analysis. The phase composition was considered as the structural basis of properties; microstructure – as a spatial expression of the phase development flow and doping consequences; hardness and modulus of elasticity – as indicators of hardening and rigidity; density – as an indicator of compaction and porosity; electrical conductivity, coefficient of thermal expansion and oxidative heat resistance – as characteristics of functional stability; and wear resistance – as a generalised result of the interaction of all these parameters in the friction mode.

The statistical stage of the study was aimed at describing the obtained values and checking the differences between the sample series. The mean value and standard deviation were determined for each indicator. The normality of the distribution was checked according to the Shapiro-Wilk criterion, and the uniformity of variances was checked according to the Leuven criterion. Differences between the three independent series were evaluated by univariate analysis of variance followed by the Tukey post hoc test. The distribution deviated from the normal one, the Kraskel-Wallis criterion with multiple pairwise comparisons was applied. The initial ordering of experimental arrays, calculation of descriptive statistics, and verification of inter-series differences were performed by Jamovi, while the construction of graphs, diagrams, and comparative visualisations was performed in GraphPad Prism 10. For each indicator – microhardness, elastic modulus, density, electrical conductivity, coefficient of linear thermal expansion, oxidation resistance, and wear parameters – generalising statistics were determined and intra-batch scattering values were estimated. The differences obtained were interpreted considering the phase composition, microstructural rearrangement, and functional properties of the material. The statistical significance level was assumed to be $p < 0.05$. In general, the applied method provided a reproducible study of the microstructural evolution of Ti-based MAX-phase alloys with various X-elements and created grounds for a holistic comparison of the structure, mechanical, thermophysical and tribological properties within a single materials science interpretation.

## Results

### Doping and phase stability of Ti-based MAX phases during X-element doping

The results of X-ray phase analysis showed that doping with different X-elements is accompanied by an unequal rearrangement of the phase composition of Ti-based MAX phases. The main differences were related to the proportion of the $Ti_3AlC_2$ phase, the intensity of carbide development, and the appearance of intermetallic components, which allows considering the phase balance as a primary structural indicator of stability or destabilisation of the layered MAX architecture. The quantitative ratio of phases in the base and doped series is shown in Table 1.

**Table 1.** Phase composition of Ti-based MAX series of phases doped with various X elements

| Sample series | Main MAX-phase $Ti_3AlC_2$, % | Carbide phases (TiC), % | Intermetallic phases, % | Other phases, % |
|---|---|---|---|---|
| Base series without doping | 87 | 10 | 0 | 3 |
| Fe doping | 62 | 28 | 7 ($Fe_3Al$) | 3 |
| Si doping | 74 | 12 | 11 ($Ti_5Si_3$) | 3 |

**Source:** created by the authors based on the results of X-ray phase analysis performed on Bruker D8 Advance with diffraction processing in HighScore Plus

As shown in Table 1, the base series without doping was characterised by the highest proportion of the $Ti_3AlC_2$ phase – 87%, which indicates the dominance of the layered MAX structure under the accepted synthesis conditions. The proportion of TiC in this series was 10%, while intermetallic components were not fixed, and other phases accounted for only 3%. This ratio indicates that in the reference material, the main MAX phase retains the role of a structural matrix, while the secondary components are limited in nature and do not determine the overall phase organisation of the alloy. In the Fe-doped series, the phase balance shifted most noticeably. The proportion of $Ti_3AlC_2$ decreased to 62%, i.e., by 25 percentage points compared to the baseline series, while the TiC content increased to 28%.

Simultaneously, the intermetallic phase $Fe_3Al$ appeared in the structure in an amount of 7%. This combination indicates a pronounced destabilisation of the layered MAX architecture, since a decrease in the proportion of the main phase is accompanied by increased carbide formation and a noticeable redistribution of components towards the intermetallic component. In phase equilibrium, this means that Fe acts as a doping element that does not support the dominance of $Ti_3AlC_2$, but stimulates the development of a more rigid, but less structurally integral carbide-intermetallic ensemble. The Si-doped series showed a different nature of phase rearrangement. The proportion of $Ti_3AlC_2$ decreased to 74%, i.e., there was also a deviation from the base composition, but it was less sharp than with Fe doping. The TiC content was 12%, and the intermetallic component was represented by the $Ti_5Si_3$ phase in the amount of 11%. In contrast to Fe doping, no sharp increase in the carbide phase was observed in this case, and the main MAX phase retained its dominant position in the structure. Such a phase balance indicates not a deep destabilisation, but a partial phase modification, in which the layered matrix is preserved, but supplemented by an interfacial intermetallic component (Kvasnytskyi *et al.*, 2020).

Comparing the three series allows distinguishing different scenarios of phase stability. The base series corresponds to a state in which $Ti_3AlC_2$ dominated, and the secondary phases have a subordinate value (Mukhamedova *et al.*, 2022). Fe doping forms a scenario of the deepest phase destabilisation, since it is accompanied by a simultaneous decrease in the proportion of the main MAX phase, a sharp increase in TiC and the appearance of $Fe_3Al$. Si doping occupied an intermediate position: it also changes the phase composition, but does not put the system in the mode of predominant carbide formation, but retains $Ti_3AlC_2$ as the main phase. It is this difference between Fe and Si that is fundamental, since it sets different trajectories for further microstructural evolution – from breaking down the lamellar architecture to partially preserving it. Taken together, the results of phase analysis showed that the nature of the doping element directly determines the degree of stability of the Ti-based MAX phase. Fe promotes the destabilisation of $Ti_3AlC_2$ and the enhanced development of carbide and intermetallic components, while Si provides a milder type of phase adjustment, in which the main MAX phase is maintained at a higher level. The established phase balance is the initial structural prerequisite for further analysis of the morphology, mechanical characteristics, thermophysical properties, and wear resistance of doped Ti-based MAX phases.

### Microstructural evolution and morphology of doped Ti-based MAX phases

The results of scanning electron microscopy, energy dispersion analysis, and digital morphometry showed that do ping with various X-elements changes the microstructural prganisation of Ti-based MAX phases not only quantitatively, but also morphologically. The degree of preservation of the lamellar architecture, the nature of interfacial boundaries, the localisation of secondary inclusions, and the average grain size were most sensitive to changes in the composition. The generalised morphometric parameters of the microstructure are shown in Table 2.

**Table 2.** Morphometric parameters of the microstructure of Ti-based MAX phases with different types of doping

| Sample series | Dominant morphology | Nature of secondary phase distribution | State of interfacial boundaries | Average grain size, μm |
|---|---|---|---|---|
| Base series without doping | Lamellar, plate | Uniform, limited | Clearly defined | 8.3 |
| Fe doping | Broken, heterogeneous, with rounded inclusions | Heterogeneous, with local concentrations of carbides and intermetallides | Partially blurred, sometimes destabilised | 5.7 |
| Si doping | Lamellar with intergranular intermetallic modification | Localised along grain boundaries | Mostly preserved, structurally ordered | 6.9 |

**Source:** formed by the authors based on the results of SEM analysis, energy dispersion analysis, and digital morphometry in Fiji

As shown in Table 2, the base series without doping was characterised by the most ordered microstructure. It was characterised by lamellar plate morphology, uniform and limited distribution of secondary phases, and well-defined interfacial boundaries. This combination of features corresponds to a structure in which the layered MAX matrix retains its integrity, and secondary components do not acquire a decisive role in the organisation of the material. Fe doping was accompanied by the deepest microstructural rearrangement. The dominant morphology lost its ordered lamellar structure and passed into a disturbed, heterogeneous state with rounded secondary inclusions. The distribution of secondary phases became heterogeneous, with local concentrations of carbides and intermetallides, and the interfacial boundaries were partially blurred and acquired signs of destabilisation. Taken together, this suggests that Fe not only changes the number of secondary phases, but also rearranges the very principle of microstructural organisation, shifting it from lamellar to a more fragmented type (Ratov *et al.*, 2023). Si doping demonstrated a different scenario of microstructural evolution. In this series, the lamellar architecture was generally preserved, although it was supplemented by an intergranular intermetallic modification. The secondary phases had a predominantly localised distribution along the grain boundaries, while the interfacial boundaries themselves remained predominantly ordered. This means that Si is not associated with the destruction of

the layered framework, but with its partial intergranular reconstruction, which preserves the overall structural integrity of the material. The change in the average grain size requires a separate comparison, since it is this indicator that quantifies the differences between the identified morphological scenarios. For a clearer comparison of morphometric differences between the series, the values of the average grain size are shown in Figure 1.

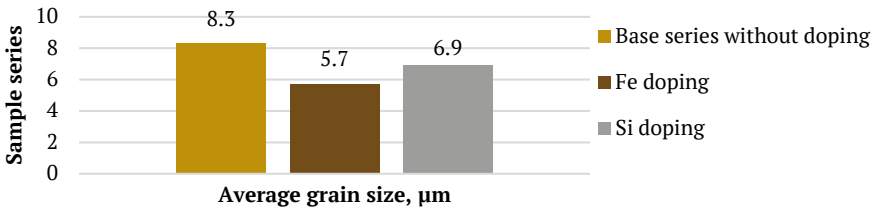


**Figure 1.** Change in the average grain size in Ti-based MAX phases when doping with various X elements
**Source:** compiled by the authors based on the results of morphometric analysis of the microstructure in Fiji

Figure 1 shows that the base series without doping had the largest average grain size – 8.3 µm. This is consistent with its most ordered lamellar morphology and well-defined interfacial boundaries. Fe doping reduced the average grain size to 5.7 µm, that is, it gave the lowest value among all the studied series. This decrease occurred simultaneously with the greatest morphological destabilisation, which indicates the grinding of the structure not as an isolated effect, but as part of the overall rearrangement associated with intensive carbide and intermetallic formation. Si doping occupied an intermediate position: the average grain size was 6.9 µm, that is, it was smaller than in the base series, but larger than in the Fe-doped material. This indicates moderate restriction of grain growth without drastic destruction of the lamellar architecture. In a comparable dimension, the data obtained reflect three different scenarios of microstructural evolution. The base series corresponds to the state with a structurally stable lamellar organisation and the largest average grain size. Fe doping forms a scenario of the deepest destabilisation, which combines grain grinding, blurring of interfacial boundaries, and heterogeneous localisation of secondary phases. Si doping occupies an intermediate position, combining grain growth restriction with relative preservation of the layered framework and ordered intergranular localisation of secondary inclusions. Thus, the results of microstructural analysis showed that the nature of the doping element determines not only the grain size, but also the type of morphological rearrangement itself, namely, this rearrangement further forms the mechanical, thermophysical and tribological properties of the doped Ti-based MAX phases.

**Effect of phase-structural adjustment on microhardness, elastic modulus, and density**

Generalisation of the results of the mechanical unit of the study showed that changes in the phase composition and microstructural organisation of Ti-based MAX phases directly affect the indicators of microhardness, elastic modulus and density. The most significant in this aspect were the differences between the series in which doping was accompanied either by destabilisation of the lamellar MAX matrix with enhanced carbide and intermetallic formation, or partial preservation of the layered architecture with intergranular modification. That is why mechanical characteristics in this subsection are considered not as isolated parameters, but as a quantitative expression of the phase-structural rearrangement of the material. A comparison of microhardness, elastic modulus, and density in the base and doped series is shown in Figure 2.

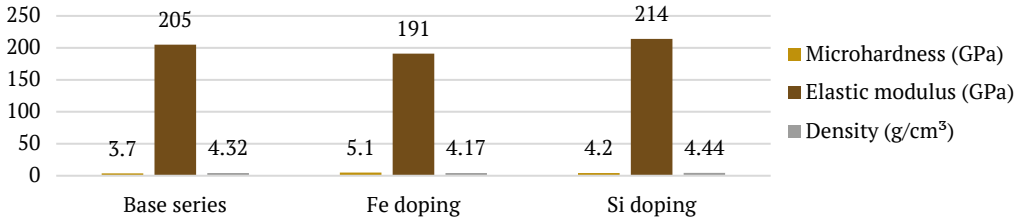


**Figure 2.** Comparison of microhardness, elastic modulus, and density in Ti-based MAX-phase series
**Source:** compiled by the authors based on the results of microhardness measurements on Buehler Micromet 5101, determination of elastic modulus on IMCE RFDA, and density estimation by the Archimedes method

Figure 2 shows that the mechanical response of Ti-based MAX phases when doping with various X elements is formed not according to a single scenario, but through different combinations of local hardening, structural rigidity, and compaction of the material. The basic series occupies a relatively balanced position: microhardness is 3.7 GPa, modulus of elasticity – 205 GPa, density – 4.32 g/cm$^3$. This corresponds to a state in which the layered MAX matrix retains structural integrity without a sharp dominance of secondary phases. The most noticeable contrast is observed

in the Fe-doped series. It shows the maximum microhardness – 5.1 GPa, but simultaneously has the lowest values of the elastic modulus – 191 GPa and density-4.17 g/cm$^3$. This combination indicates that Fe increases the local indentation resistance, which is consistent with an increase in the proportion of TiC and the appearance of $Fe_3Al$, but this strengthening is achieved not through structural ordering, but through a more rigid and simultaneously less integral carbide-intermetallic framework. A decrease in density indicates a lower degree of compaction and a higher probability of porosity or defect, and a decrease in the elastic modulus indicates a weakening of the continuity of the layered matrix despite an increase in hardness. The Si-doped series demonstrates a different type of mechanical response. The microhardness here is 4.2 GPa, i.e., it exceeds the base series, but remains lower than the Fe-doped variant. This particular series has the highest modulus of elasticity – 214 GPa and the highest density – 4.44 g/cm$^3$. This distribution of indicators indicates that Si does not provide maximum local hardening, but provides a more favourable combination of rigidity and structural compaction. This is in good agreement with previous phase and microstructural results, where Si was associated with less drastic destabilisation of $Ti_3AlC_2$ and more ordered intergranular modification. An increase in microhardness does not in itself mean an improvement in the entire complex of mechanical properties (Adjamskiy *et al.*, 2022). Fe doping forms a local hardening scenario against the background of structural destabilisation, while Si doping provides a more balanced mechanical profile with increased stiffness and density. In this sense, the mechanical response of Ti-based MAX phases is determined not by a single indicator, but by a cumulative phase-structural rearrangement, which is implemented differently depending on the nature of the doping element. That is, the mechanical response of Ti-based MAX phases is determined not by one single parameter, but by a cumulative rearrangement of the phase composition, morphology, and interfacial organisation. An increase in microhardness is accompanied by various structural scenarios: in the case of Fe – carbide-intermetallic hardening with loss of part of the structural integrity, in the case of Si – moderate hardening against the background of maintaining a more ordered lamellar base. Density in this context reflects not only the degree of compaction, but also the general nature of the microstructural organisation, in particular, the relationship between the preservation of the matrix phase and the development of secondary inclusions. Consequently, the results of mechanical analysis confirm that phase-structural rearrangement determines not only the local strain resistance, but also the overall level of rigidity and structural integrity of doped Ti-based MAX phases.

**Thermophysical and functional properties of doped Ti-based MAX phases**

The results of the thermophysical and functional unit of the study showed that doping with various X-elements changes not only the phase and microstructural state of the Ti-based MAX phases, but also the method of thermal and electrical response of the material under thermal load conditions. Electrical conductivity, coefficient of linear thermal expansion, and oxidative heat resistance were the most sensitive to phase-structural adjustment, while thermal conductivity was considered as an integral indicator, the value of which was determined by the preservation or violation of the layered architecture, the state of grain boundaries, and the spatial distribution of secondary phases. Table 3 summarises the thermophysical and functional characteristics of the base and doped series of Ti-based MAX phases.

**Table 3.** Thermophysical and functional characteristics of Ti-based MAX phases when doping with various X elements

| Sample series | Electrical conductivity, S/m | Coefficient of linear thermal expansion, $\times 10^{-6}$ 1/°C | Mass loss based on thermogravimetric analysis, % |
|---|---|---|---|
| Base series without doping | $3.5 \times 10^4$ | 8.1 | 5.8 |
| Fe doping | $2.1 \times 10^4$ | 9.7 | 8.6 |
| Si doping | $3.2 \times 10^4$ | 7.5 | 3.4 |

**Source:** created by the authors based on the results of electrical conductivity measurements on Loresta GP MCP-T610, dilatometric analysis on Linseis L75 PT, and thermogravimetric analysis on Netzsch STA 449 F3 Jupiter

As shown in Table 3, the base series without doping was characterised by the most balanced combination of functional parameters. The electrical conductivity was $3.5 \times 10^4$ S/m, the coefficient of linear thermal expansion was $8.1 \times 10^{-6}$ 1/°C, and the mass loss according to the results of thermogravimetric analysis was 5.8%. This ratio corresponds to a structure in which $Ti_3AlC_2$ retains its dominant position, and the secondary phases do not critically disrupt either the conducting paths or the stability of the material when heated. In a functional sense, the base series sets a reference level relative to which the area and depth of changes caused by doping can be estimated. The Fe-doped series showed the least favourable complex of thermophysical and functional characteristics. The electrical conductivity was reduced to $2.1 \times 10^4$ S/m, i.e., a significant part of the conductivity was lost compared to the base series. The coefficient of linear thermal expansion increased to $9.7 \times 10^{-6}$ 1/°C, and the mass loss for TGA reached 8.6%, which is the maximum value among the studied series. This combination of indicators is

consistent with the previously established phase-structural destabilisation: an increase in the proportion of TiC, the appearance of $Fe_3Al$, a decrease in the average grain size and blurring of interfacial boundaries form a more heterogeneous environment for charge and heat transfer, and simultaneously reduce resistance to high-temperature oxidation. Consequently, Fe doping is accompanied not only by a rearrangement of the phase composition, but also by a systemic deterioration in the functional profile of the material. The Si-doped series, on the contrary, showed the most stable type of thermophysical behaviour. The electrical conductivity in it was $3.2 \times 10^4$ S/m, that is, it remained close to the base series, the coefficient of linear thermal expansion decreased to $7.5 \times 10^{-6}$ 1/°C, and the mass loss by TGA was minimal – 3.4%. Taken together, this indicates that SI doping does not lead to deep destruction of the conductive framework of the MAX matrix, but, on the contrary, is associated with higher dimensional stability and better resistance to oxidative degradation. Figure 3 summarises the thermogravimetric curves of the base and doped series of Ti-based MAX phases, which allows comparing not only the final level of degradation, but also the course of the oxidation process over the entire temperature range.

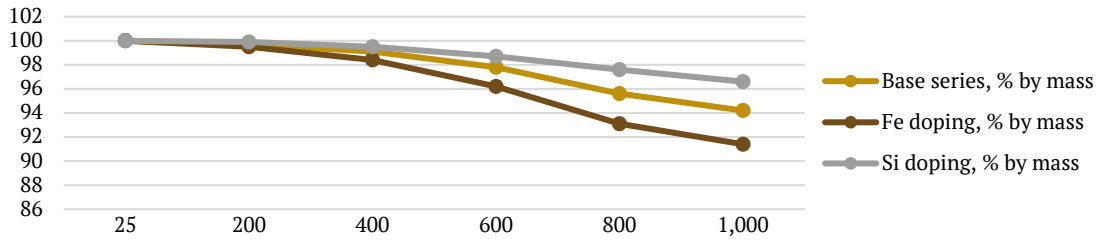


**Figure 3.** Change in the mass of Ti-based MAX-phase samples based on the results of thermogravimetric analysis

**Source:** created by the authors based on the results of thermogravimetric analysis performed on a Netzsch STA 449 F3 Jupiter

As can be seen from Figure 3, the change in the mass of the samples during heating occurred in different scenarios depending on the type of doping, and the differences between the series were observed not only in the final mass loss, but also in the course of the thermogravimetric process itself. The base series showed a moderate decrease in residual mass as the temperature increased: at the initial heating sites, the changes are insignificant, while in the region of higher temperatures, the degradation becomes more intense and up to 1,000°C, the residual mass decreases to 94.2%. Such a curve corresponded to a material with a relatively stable phase base, but without additional factors that would significantly restrain the oxidation processes at the final stages of heating. The Fe-doped series showed the least stable behaviour. Already in the intermediate temperature sections, its curve passed below the base one, and in the region of high temperatures, the mass decline became the most pronounced. By 1,000°C, the residual mass decreased to 91.4%, which corresponds to the maximum loss among all the studied series. This nature of the curve indicates that Fe doping not only increases the overall level of oxidative degradation, but also makes the mass loss process more intense over the entire temperature range. In a structural sense, this is consistent with the greatest phase and microstructural destabilisation established earlier: an increase in the proportion of TiC, the appearance of $Fe_3Al$, grain grinding, and a violation of the lamellar architecture, which creates a less stable material when heated. The Si-doped series, on the contrary, is characterised by the wettest curve and the smallest decrease in residual mass. Throughout the entire temperature range, its values remained higher than those of the base and Fe-doped series, and at 1,000°C, the residual mass is 96.6%. This indicates that Si doping provides the highest oxidative heat resistance among the studied variants. It is important to note that this behaviour was observed not only at the end point, but throughout the heating process, i.e., Si is associated not with a local, but with a systemic slowdown in degradation processes. The results confirmed that the type of doping element determines not only the final level of mass loss, but also the shape of the thermogravimetric response of the material. Fe doping established a scenario of accelerated oxidative degradation, the base series retained an intermediate behaviour, while Si doping formed the most stable curve with minimal mass loss.

**Wear resistance and wear mechanisms of Ti-based MAX phases in dry friction mode**

The results of tribological tests showed that the behaviour of Ti-based MAX phases in the dry friction mode is determined not by a separate mechanical indicator, but by the integral action of the phase composition, microstructural organisation, hardness, density, and thermophysical stability of the material. It is in the tribological mode that it is most clearly shown how much the structural adjustment caused by doping is favourable or, conversely, destabilising from the standpoint of the actual operational response of the material. To compare the base and doped series, Figure 4 summarises the indicators of mass loss, wear value, and coefficient of friction, which allows estimating wear resistance as the final result of the entire pre-set phase-structural and functional evolution.

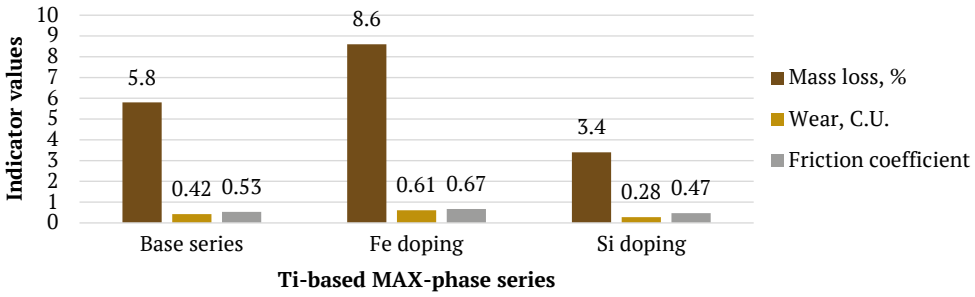


**Figure 4.** Comparison of mass loss, wear and coefficient of friction indicators in the base and doped Ti-based MAX phase series

**Source:** compiled by the authors based on the results of tribological tests in the dry friction mode and subsequent statistical processing in Jamovi and GraphPad Prism 10

Figure 4 showed that the tribological behaviour of Ti-based MAX phases is determined by the combined effect of phase composition, microstructure, and functional characteristics, not just the level of hardness. The base series occupied an intermediate position in all three indicators: mass loss was 5.8%, wear – 0.42 C.U., the coefficient of friction – 0.53. This distribution corresponds to a relatively stable lamellar structure dominated by $Ti_3AlC_2$, which provided moderate wear resistance without a pronounced tribological advantage. The Fe-doped series occupied the least favourable position: it was characterised by the greatest mass loss – 8.6%, maximum wear – 0.61 C.U. and the highest coefficient of friction – 0.67. This indicates that the increase in microhardness was not accompanied by an increase in wear resistance. This discrepancy is associated with phase-structural destabilisation, since the growth of the proportion of TiC and $Fe_3Al$, grain grinding, and inhomogeneity of the interfacial space formed a rigid but less integral surface layer. The Si-doped series, on the contrary, occupied the best position in terms of tribological indicators. For it, the minimum values of mass loss were recorded – 3.4%, wear – 0.28 C.U. and the coefficient of friction – 0.47. This indicates that SI doping provided the most stable surface layer in the dry friction regime, which is consistent with better preservation of the lamellar architecture, ordered grain boundaries, and generally a more balanced structural and functional state of the material (Baklanov *et al.*, 2022).

Thus, the results of tribological analysis showed that the highest wear resistance is demonstrated by the Si-doped series, which is characterised by the most balanced combination of phase composition, microstructural organisation, rigidity, density, and thermal stability. It is in this series that the higher content of the main phase $Ti_3AlC_2$ is preserved, the lamellar architecture is less disturbed, and the secondary phases are localised in a more orderly manner, without deep destabilisation of the interfacial space. As a result, the surface layer works more stably during friction, is less susceptible to discolouration and better counteracts the accumulation of local damage, which is reflected in the minimum values of mass loss, wear and coefficient of friction. The base series retains an intermediate level of wear resistance, which is conditioned by the relatively ordered layered structure and the dominance of $Ti_3AlC_2$, but without the additional structural effect that would increase the wear resistance. Such a material does not show a sharp destabilisation, but it does not form the optimal combination of rigidity, compaction and thermal stability that is observed during Si doping (Malecha *et al.*, 2025). Therefore, its tribological behaviour is more stable than as effective as possible. Fe doping, despite the increase in microhardness, is accompanied by less favourable tribological behaviour due to deeper phase-structural destabilisation. An increase in the proportion of TiC and $Fe_3Al$, a decrease in the average grain size, a heterogeneous distribution of secondary phases, and a partial violation of interfacial boundaries form a microstructure in which local hardening is combined with a decrease in overall structural integrity. In the dry friction mode, this is manifested in unstable contact, an increased tendency to micro-destruction of the surface layer, and a worse agreement between hardness and actual wear resistance. That is, Fe increases the resistance to local indentation, but does not provide stable resistance to surface destruction (Shevko *et al.*, 2020). As a result, it is the nature of microstructural rearrangement that determines whether doping is transformed into an increase in operational stability, or, conversely, into an increase in the tendency to surface destruction in the dry friction mode. For Ti-based MAX phases, the principle is not the maximum increase in a particular mechanical parameter, but the preservation of structural order, controlled development of secondary phases, and stability of the surface layer under load. That is why the most promising type of doping from the standpoint of tribological application is that which does not destroy the layered MAX framework, but modifies it without losing its structural integrity (Nedeva, 2025).

In general, the results obtained showed that doping of Ti-based MAX phases with different X elements sets not just differences in individual indicators, but different scenarios for the structural and inherent evolution of the material. The base series retained the most stable layered MAX architecture with $Ti_3AlC_2$ dominance, moderate mechanical characteristics, balanced thermophysical parameters, and intermediate wear resistance. Fe doping caused the deepest phase and microstructural destabilisation, which was manifested in a decrease in the proportion of $Ti_3AlC_2$, an increase in TiC and $Fe_3Al$, grain grinding,

disruption of lamellar organisation, and the development of a heterogeneous interfacial space. This led to a local increase in microhardness, but also was accompanied by a decrease in elastic modulus, density, electrical conductivity, deterioration of thermal stability, and the least favourable tribological behaviour. Si doping, on the contrary, provided a more controlled type of phase modification: while maintaining the dominance of $Ti_3AlC_2$ and the development of $Ti_5Si_3$ in the intergranular space, the structure remained more ordered, the grain organisation – more stable, and the complex of mechanical, thermophysical and tribological characteristics – the most balanced. That is why the Si-doped series demonstrated the highest wear resistance, the best oxidation heat resistance and the most favourable combination of rigidity, density, and functional stability. Thus, the key factor in the operational efficiency of Ti-based MAX phases was not the maximum increase in a particular property, but the type of microstructural adjustment that determines whether the integrity of the layered MAX frame is preserved under mechanical, thermal, and tribological loads.

## Discussion

The complex of established regularities showed that doping of Ti-based MAX phases changed not one individual characteristic, but the entire chain "phase composition-microstructure – mechanical response – functional stability – wear resistance". This logic fits well with the advanced concept of materials engineering, where the operational effect is determined not by local reinforcement itself, but by the way structural modification rearranges the behaviour of the material under load conditions. The generalised emphasis on the role of complex control of the structure and surface state of the material echoed the conclusions of H. Sun *et al*. (2025), where advanced coating technologies were considered as a tool for purposeful development of durability, wear resistance, and stability of properties. This statement corresponded to the dependence found here, in which it was the nature of phase-microstructural rearrangement that determined whether the operational profile of the Ti-based MAX phase improved or, conversely, became less stable.

The contrast between local reinforcement and overall structural integrity correlated well with the results of W. Maziarz *et al*. (2024), where TiC-containing nanocomposites also showed increased stiffness due to solid secondary phases. However, such rigidity was not considered as a self-sufficient advantage, since the properties were also determined by how homogeneous the microstructural organisation remained, which conceptually coincided with the less favourable behaviour of the Fe-doped series. The milder and structurally controlled modification scenario was consistent with the observations of T. Ma *et al*. (2022), where $Ti_2AlC$-containing composites were interpreted as systems in which reinforcement is achieved without destroying the base frame of the material. This logic was also traced here: Si doping did not put the system in the deepest destabilisation mode, but retained the dominant role of the MAX phase while simultaneously improving the complex of properties. The role of interfaces and phase boundaries in the development of the mechanical response was consistent with the study by Y. Zhou *et al*. (2023), where the properties of laminated Ti/Al composites were directly related to the state of interfacial interaction. This parallel was also important for Ti-based MAX phases, since it was the nature of grain boundaries and the way secondary phases were localised that distinguished the destabilised Fe-containing variant from the more ordered Si-modified state. The emphasis on the spatial organisation of reinforcement phases echoed the conclusions of Z. Yuan *et al*. (2022), where the properties of titanium composites were determined not only by the presence of reinforcing components, but also by their distribution in the matrix and structural uniformity. In this sense, the heterogeneous interfacial space during Fe doping and intergranular localised modification during Si doping corresponded to two different scenarios of evolution, which led to differences in mechanical and tribological behaviour. A favourable combination of rigidity and functional stability found a conceptual parallel in the results of S. Zhou *et al*. (2026), where Cu-$Ti_3AlC_2$ composites were considered as systems with structural synergy between the MAX phase and the matrix. A close emphasis was also observed here, since the best property profile was implemented not where the solid phases were most abundant, but where a more consistent structural organisation of the entire system was preserved. The fact that wear resistance was determined not only by the hardness, but also by the stability of the surface layer correlated with the results of X. Zeng *et al*. (2022), where the tribological efficiency of self-lubricating coatings was related to the combination of composition, microstructure, and contact mode. This is why the highest microhardness of the Fe-doped series did not translate into better wear resistance, while the Si-containing material showed more stable behaviour under dry friction conditions.

The idea of the importance of preserving a MAX-like framework was consistent with the results of L. Cao *et al*. (2024), where high-entropy ceramics $(TiVNbTaM)_2AlC$ were interpreted as systems in which the composition was significant primarily due to the effect on the structural stability of the MAX phase. This formulation was consistent with the distinction found here between Fe doping as a destabilisation scenario and Si doping as a more controlled phase modification scenario. The balance between the MAX phase and the carbide component resonated well with the paper by A. Deng *et al*. (2025), where the properties of $M_2AlC$-MC composites were explained precisely by the ratio of the matrix MAX phase and rigid carbides. In this context, the unfavourable profile of the Fe-doped material was associated not only with the presence of TiC, but also with the fact that the carbide and intermetallic components began to displace the structure-forming role of $Ti_3AlC_2$. The dependence of oxidation resistance on the method of phase modification correlated with the results of Y. Xu *et al*. (2025), where an increase in oxidation resistance in $Ti_2AlC$ was achieved through solid solutions that

suppressed degradation processes. A similar emphasis was observed here: the wettest thermogravimetric curve and the lowest mass loss during Si doping indicated systemically higher stability, rather than the local effect of a single phase. A similar logic was also reflected in the paper by A. Zhang *et al*. (2024), where an improvement in the oxidative stability of $Ti_2AlC$ coatings was associated with modification without destruction of the base MAX framework. It was this interpretation that corresponded to the conclusion established here that the most promising type is the type of doping that does not destabilise the layered architecture, but modifies it while maintaining structural integrity. Further development of the tribological block was in good agreement with the results of L. Cai *et al*. (2024), where the effect of solid-soluble elements on $Ti_3AlC_2$ was considered due to the self-lubricating effect and temperature-dependent friction stability over a wide range. This statement directly echoed the fact found here that favourable tribological behaviour was determined not only by the hardness, but also by the ability of the structurally modified MAX-phase to maintain a stable contact regime and restrain progressive surface destruction. A close accent could be traced in the paper by J. Li *et al*. (2024), where a-site doping of $Ti_3AlC_2$ was interpreted as a factor altering the tribological response by rearranging the MAX structure itself, rather than simply increasing the strength. This corresponded to the pattern established here, in which the type of doping element determined whether the structural modification turned into an increase in wear resistance, or, conversely, into an increase in the tendency to surface destruction.

The role of $Ti_3AlC_2$ as a structurally active component capable of changing the microhardness and tribological characteristics of the composite system correlated with the results of V. Desai *et al*. (2025), where Al7075/$Ti_3AlC_2$ surface composites after friction stir processing were also interpreted through a combination of microstructural rearrangement, local hardening, and changes in the friction mode. This logic also corresponded to the distinction found here between local reinforcement and integral wear resistance, since the very fact of the presence of the MAX phase was important only if its structurally favourable integration. A similar parallel was traced in the paper by M. Li *et al*. (2026), where $Ti_3AlC_2$ as an additive to WC-Co hard alloys simultaneously affected the mechanical and tribological characteristics of the system. This conceptually coincided with the dependence established here, in which the MAX-containing component did not act in isolation, but through a change in the entire structural and inherent profile of the material, including contact stability under friction. The oxidative behaviour of the established series correlated well with the results of S. Badie *et al*. (2021), where for $Ti_2AlC$, the breakaway oxidation mechanism was explained by a change in the structural state of the surface layer and a violation of its protective function. This statement was consistent with the fact that the deterioration of oxidative heat resistance during Fe doping reflects not only a greater mass loss, but also a deeper instability of the structural phase state during heating.

A more applied parallel to the behaviour of MAX phases in the form of coatings was observed in N. Laska *et al*. (2024), where the oxidation of $Ti_2AlC$-based coatings on γ-TiAl was also interpreted due to the relationship between the microstructure, the stability of the MAX component, and the preservation of the protective properties of the system. This was consistent with the conclusion established here that better oxidative stability was realised where a more ordered structural framework and controlled localisation of secondary phases were preserved. Tribological consequences of the introduction of $Ti_2AlC$ as a strengthening component found a parallel in S.W. Hua *et al*. (2023), where $Ti_2AlC$-reinforced coatings on Ti6Al4V showed a change in wear resistance due to the microstructural organisation and the nature of particle distribution in the Matrix. This emphasis directly echoed the relationship found in this study, in which it was the type of distribution of secondary phases and the degree of preservation of the layered architecture that determined whether the tribological effect would be favourable. The functional aspect related to electrical conductivity correlated with the results of M. Mandegari *et al*. (2023), where the dual MAX-phase $Ti_3AlC_2$-$Ti_2AlC$ system was interpreted as a material with high electrical conductivity due to the preservation of a structurally favourable phase coupling. This was consistent with the fact established here that a more stable MAX framework during Si doping was accompanied by preservation of electrical conductivity, while deeper phase-microstructural destabilisation during Fe doping led to its noticeable decrease. The temperature stability of the MAX phases over a wider heating range was consistent with the conclusions of M. Potoczek *et al*. (2023), where the oxidative behaviour of $Ti_2AlC$ MAX-phase foams in the range of 600-1,000°C also depended on the structural features and course of degradation processes with increasing temperature. A similar logic was also traced here, since the shape of the thermogravimetric curve was just as important as the final mass loss, and the most stable scenario was associated with a more ordered structural state of the Si-doped series. As a result, comparison with the sources confirmed that for Ti-based MAX phases, the decisive factor is not the increase in a particular property, but the type of structural modification that simultaneously determines oxidative stability, conductivity, and behaviour under friction conditions. That is why the compositional scenario in which doping did not destroy the MAX framework, but provided its controlled modification while maintained a complete microstructural organisation remained the most promising.

## Conclusions

As part of the study, it was found that doping of Ti-based MAX phases with various X elements determines not isolated changes in individual parameters, but integral scenarios of phase-microstructural evolution, which directly form the mechanical, thermophysical and tribological characteristics of the material. X-ray phase analysis showed that the baseline series retains the dominance of $Ti_3AlC_2$ at 87%, while Fe doping reduces its proportion to 62% and is

accompanied by increased carbidisation (TiC – 28%) and the appearance of $Fe_3Al$ (7%), which corresponds to the scenario of the deepest phase destabilisation. Si doping, on the contrary, forms a milder type of phase modification: the proportion of $Ti_3AlC_2$ remains at 74%, TiC is 12%, and the appearance of $Ti_5Si_3$ (11%) does not put the system in the dominant carbide formation mode. Microstructural analysis confirmed that the base series is characterised by the most ordered lamellar organisation with clear interfacial boundaries and an average grain size of 8.3 μm, while Fe doping is accompanied by the most pronounced morphological destabilisation, grain grinding up to 5.7 μm, heterogeneous distribution of secondary phases, and partial blurring of boundaries.

In the Si-doped series, the lamellar architecture is preserved with intergranular intermetallic modification and an intermediate average grain size of 6.9 μm, which indicates a restriction of grain growth without deep destruction of the structural framework. The mechanical unit of the study showed that Fe doping provides a maximum microhardness of 5.1 GPa, but is also accompanied by a decrease in the elastic modulus to 191 GPa and density to 4.17 g/cm$^3$, that is, local hardening is implemented against the background of general structural destabilisation. Si doping forms a different type of mechanical response: with a moderate microhardness of 4.2 GPa, it provides maximum values of the elastic modulus of 214 GPa and a density of 4.44 g/cm$^3$, which indicates a more favourable combination of rigidity and compaction. Thermophysical and functional analysis showed that the Fe-doped series has the least favourable profile: the conductivity decreases to $2.1 \times 10^4$ S/m, the coefficient of linear thermal expansion increases to $9.7 \times 10^{-6}$ 1/°C, and the mass loss by TGA reaches 8.6%, which indicates the lowest oxidative heat resistance. Si doping, on the contrary, provides the most stable functional state: the electrical conductivity is $3.2 \times 10^4$ S/m, the coefficient of linear thermal expansion was reduced to $7.5 \times 10^{-6}$ 1/°C, and the mass loss by TGA was limited to 3.4%, which corresponds to the best resistance to oxidative degradation. Tribological tests in the dry friction mode confirmed that wear resistance is determined not by the hardness level itself, but by the aggregate structural organisation of the material: the Fe-doped series, despite the highest microhardness, showed the greatest mass loss of 8.6%, maximum wear of 0.61 C.U. and the highest coefficient of friction – 0.67, while the Si-doped series showed a minimum mass loss of 3.4%, wear of 0.28 C.U., and the coefficient of friction – 0.47.

Thus, the results proved that the least favourable scenario for Ti-based MAX phases is associated with Fe doping, which enhances the carbide-intermetallic rearrangement, destabilises the lamellar architecture, and degrades the complex of mechanical, thermophysical, and tribological characteristics. The most balanced structural and functional profile is formed by Si doping, which provides partial preservation of $Ti_3AlC_2$, more ordered intergranular organisation, high rigidity, better oxidative heat resistance, and the highest wear resistance. Thus, the key factor in the operational efficiency of Ti-based MAX phases was not the maximum increase in a particular property, but the type of microstructural adjustment that determines whether the integrity of the layered MAX frame is preserved under mechanical, thermal and tribological loads.

Further research should be aimed at expanding a number of doping X-elements, varying their concentrations, clarifying the mechanisms of intergranular stabilisation, and checking the behaviour of Ti-based MAX phases in more complex modes of thermocyclic and tribocorrosive loading, characteristic of drilling and hydrocarbon production conditions.

## Acknowledgements

None.

## Funding

None.

## Conflict of Interest

None.

## References

[1] Adjamskiy, S., Kononenko, G., Podolskyi, R., & Baduk, S. (2022). Studying the influence of orientation and layer thickness on the physico-mechanical properties of Co-Cr-Mo alloy manufactured by the SLM method. *Science and Innovation*, 18(5), 85-94. doi: 10.15407/scine18.05.085.

[2] Aghajanyan, N.N., Dolukhanyan, S.K., Ter-Galstyan, O.P., Muradyan, G.N., & Hovhannisyan, A.A. (2023). Self-propagating high-temperature synthesis of MAX phases in Ti-Zr-Al-C system (C: P15). *Ceramics International*, 49(14), 24165-24170. doi: 10.1016/j.ceramint.2022.11.041.

[3] Aydinyan, S. (2023). Combustion synthesis of MAX phases: Microstructure and properties inherited from the processing pathway. *Crystals*, 13(7), article number 1143. doi: 10.3390/cryst13071143.

[4] Badie, S., Sebold, D., Vaßen, R., Guillon, O., & Gonzalez-Julian, J. (2021). Mechanism for breakaway oxidation of the $Ti_2AlC$ MAX phase. *Acta Materialia*, 215, article number 117025. doi: 10.1016/j.actamat.2021.117025.

[5] Baklanov, V., Zhanbolatova, G., Skakov, M., Miniyazov, A., Sokolov, I., Tulenbergenov, T., Kozhakhmetov, Y., Bukina, O., & Orazgaliev, N. (2022). Study of the temperature dependence of a carbidized layer formation on the tungsten surface under plasma irradiation. *Materials Research Express*, 9(1), article number 016403. doi: 10.1088/2053-1591/ac4626.

[6] Berrabah, M., Cabioc'h, T., Brunet, V.G., Chartier, P., Epifano, E., & Dubois, S. (2025). Synthesis, microstructural characterization and transport properties of a new $(Ti_2Nb)AlC_2$ ternary nanolaminate carbide solid solution. *Journal of the European Ceramic Society*, 46(3), article number 117894. doi: 10.1016/j.jeurceramsoc.2025.117894.

[7] Cai, L., Li, J., Luo, B., Yang, J., He, N., & Jia, J. (2024). Self-lubricating effect of solid solution elements on tribological performance of $Ti_3AlC_2$ over a wide temperature range. *Journal of the American Ceramic Society*, 107(5), 3103-3116. doi: 10.1111/jace.19662.

[8] Cao, L., Zhang, Q., Du, L., Fu, S., Wan, D., Bao, Y., Feng, Q., & Hu, C. (2024). Synthesis and characterization of high entropy $(TiVNbTaM)_2AlC$ (M=Zr, Hf) ceramics. *Journal of Advanced Ceramics*, 13(2), 237-246. doi: 10.26599/JAC.2024.9220847.

[9] Deng, A., Niu, Y., Zhang, B., Lin, N., Ma, C., Huang, Z., & Yin, J. (2025). Synthesis, microstructure and mechanical properties of $M_2AlC$-MC (M = Ti, Ta, Nb) composite. *Journal of Alloys and Compounds*, 1014, article number 178745. doi: 10.1016/j.jallcom.2025.178745.

[10] Desai, V., Badheka, V., Zala, A., Parekh, T., & Jamnapara, N.I. (2025). Al7075/$Ti_3AlC_2$ MAX-phase surface composite generated by friction stir processing: Microstructure, microhardness, and tribological characteristics. *Tribology-Materials, Surfaces & Interfaces*, 19(4), 265-276. doi: 10.1177/17515831251358689.

[11] Gui, X., Sun, L., Chen, C., Yang, Y., Gao, W., Gyawali, G., Liu, X., Ding, J., & Zhang, S. (2025). Optimizing current-carrying tribological performance of Cu-$Ti_2AlC$ coatings: Role of kerosene flow rate in HVOF spraying and wear mechanism analysis. *Tribology International*, 111377. doi: 10.1016/j.triboint.2025.111377.

[12] Hong, H., Yang, P., Gui, X., Yang, Y., Liu, X., Ding, J., Gyawali, G., Yang, K., & Zhang, S. (2025). Enhancing the durability of Ti-Al-C coatings: The role of powder composition and processing variables. *Journal of Materials Research and Technology*, 34, 2956-2963. doi: 10.1016/j.jmrt.2024.12.226.

[13] Hua, S.W., Pang, M., Chen, J., Zhao, J., & Ji, F.Q. (2023). Microstructure and tribological performance of laser cladding $Ti_2AlC$ particle reinforced coatings on Ti6Al4V. *Journal of Materials Engineering and Performance*, 32(18), 8452-8466. doi: 10.1007/s11665-022-07714-3.

[14] Kvasnytskyi, V., Korzhyk, V., Kvasnytskyi, V., Mialnitsa, H., Dong, C., Pryadko, T., Kurdyumov, G.V., Matviienko, M., & Buturlia, Y. (2020). Designing brazing filler metal for heat-resistant alloys based on NI3AL intermetallide. *Eastern-European Journal of Enterprise Technologies*, 6(12), 6-19. doi: 10.15587/1729-4061.2020.217819.

[15] Laska, N., Swadźba, R., Nellessen, P., Helle, O., & Anton, R. (2024). Oxidation behavior of $Ti_2AlC$ MAX phase-based coating on a γ-TiAl alloy TiAl48-2-2 produced by DC magnetron sputtering. *Surface and Coatings Technology*, 480, article number 130601. doi: 10.1016/j.surfcoat.2024.130601.

[16] Li, M., Wei, D., Gong, M.F., Guo, Z.Y., Mo, D.Y., & Wu, W.G. (2026). Effect of $Ti_3AlC_2$ as an additive on the mechanical and tribological properties of WC-Co cemented carbide. *Strength of Materials*, 57, 1260-1271. doi: 10.1007/s11223-026-00855-z.

[17] Liu, B., Zhang, C., Su, Y.F., Tang, P., Kuang, T.C., Lin, S.S., & Shi, Q. (2026). In situ induced Ti-C composite interlayer for enhanced corrosion resistance and electrical conductivity in a-C: Ti films on SS316L bipolar plates. *SSRN*. doi: 10.2139/ssrn.6017176.

[18] Lu, Y., Peng, Y., Chang, X., & Kong, D. (2024). $Ti_2AlC$ and $Ti_3AlC_2$ reinforced CoNi coatings by laser cladding: Nanostructures, tribological properties and density functional theory calculations. *Journal of Manufacturing Processes*, 131, 736-749. doi: 10.1016/j.jmapro.2024.09.031.

[19] Ma, T., Li, Q., Wang, Y., Wang, X., Dong, D., & Zhu, D. (2022). Microstructure and mechanical properties of micro-nano $Ti_2AlC$-reinforced TiAl composites. *Intermetallics*, 146, article number 107563. doi: 10.1016/j.intermet.2022.107563.

[20] Malecha, D., Zubko, M., Żabiński, P., & Małecki, S. (2025). Analysis of the lead refining method using aluminium. *Metallurgical and Materials Transactions A: Physical Metallurgy and Materials Science*, 56(8), 2957-2975. doi: 10.1007/s11661-025-07813-5.

[21] Mandegari, M., Nasouri, K., & Ghasemi-Mobarakeh, L. (2023). Synthesis of low-cost $Ti_3AlC_2$-$Ti_2AlC$ dual MAX phase with high-electrical conductivity using economical raw materials and novel compositions. *Materials Today Communications*, 36, article number 106868. doi: 10.1016/j.mtcomm.2023.106868.

[22] Maziarz, W., Wójcik, A., Chulist, R., Bigos, A., Kurtyka, P., Szymański, Ł., Jimenez Zabaleta, A., García de Cortázar, M., & Olejnik, E. (2024). Microstructure and mechanical properties of Al/TiC and Al/(Ti,W)C nanocomposites fabricated via in situ casting method. *Journal of Materials Research and Technology*, 28, 1852-1863. doi: 10.1016/j.jmrt.2023.12.126.

[23] Mukhamedova, N., Kozhakhmetov, Y., Skakov, M., Kurbanbekov, S., & Mukhamedov, N. (2022). Microstructural stability of a two-phase (O + B2) alloy of the Ti-25Al-25Nb system (at.%) during thermal cycling in a hydrogen atmosphere. *AIMS Materials Science*, 9(2), 270-282. doi: 10.3934/MATERSCI.2022016.

[24] Muradyan, G.N., Dolukhanyan, S.K., Aleksanyan, A.G., Ter-Galstyan, O.P., Mnatsakanyan, N.L., Asatryan, K.V., Mardanyan, S.S., & Hovhannisyan, A.A. (2023). Synthesis in hydride cycle of Ti-Al-C based MAX phases from mixtures of titanium carbohydrides and aluminium powders. *Ceramics International*, 49(14), 24171-24178. doi: 10.1016/j.ceramint.2022.11.125.

[25] Nedeva, D. (2025). Preparation, properties, and application of titanium carbide coatings. *Zeitschrift für Naturforschung A*, 80(10), 993-1008. doi: 10.1515/zna-2025-0152.

[26] Potoczek, M., Dąbek, J., & Brylewski, T. (2023). Oxidation behavior of $Ti_2AlC$ MAX-phase foams in the temperature range of 600-1000°C. *Journal of Thermal Analysis and Calorimetry*, 148(10), 4119-4127. doi: 10.1007/s10973-023-11990-z.

[27] Ratov, B.T., *et al*. (2023). Features structure of the $C_{diamond}$-(WC-Co)-$ZrO_2$ composite fracture surface as a result of impact loading. *Journal of Superhard Materials*, 45(5), 348-359. doi: 10.3103/S1063457623050088.

[28] Shahbaz, M., Sabir, N., Amin, N., Zulfiqar, Z., & Zahid, M. (2024). Synthesis and characterization of chromium aluminium carbide MAX phases (CrxAlCx-1) for potential biomedical applications. *Frontiers in Chemistry*, 12, article number 1413253. doi: 10.3389/fchem.2024.1413253.

[29] Shevko, V.M., Karataeva, G.E., Badikova, A.D., Tuleev, M.A., & Uteeva, R.A. (2020). Comprehensive processing of basalt together with magnetite concentrate in order to obtain ferrous alloy and calcium carbide. *Archives of Foundry Engineering*, 20(4), 41-54. doi: 10.24425/afe.2020.133346.

[30] Sun, H., Song, B., Sun, X., Cui, X., Liu, Z., Cong, M., & Wang, L. (2025). Recent representative progress of surface coating technology. *The Chemical Record*, 25(8), article number e202500054. doi: 10.1002/tcr.202500054.

[31] Wu, H., Xiao, H., Chen, N., Chu, M., Lin, B., Zhang, Z., Fu, G., & Mo, T. (2025). Effect of Nb content on the tribological properties of laser-cladded Ti-Al-C MAX phase composite coatings. *Tribology International*, 204, article number 110426. doi: 10.1016/j.triboint.2024.110426.

[32] Xu, Y., Ma, G., Li, Z., Zhang, Y., Zhang, A., Wang, Z., & Wang, A. (2025). Valence-dependent $TiO_2$ inhibition for enhancing oxidation resistance in $Ti_2AlC$ via Zr/Nb solid solution. *Corrosion Science*, 257, article number 113351. doi: 10.1016/j.corsci.2025.113351.

[33] Yuan, Z., Liu, H., Ma, Z., Ma, X., Wang, K., & Zhang, X. (2022). Microstructure and properties of high entropy alloy reinforced titanium matrix composites. *Materials Characterization*, 187, article number 111856. doi: 10.1016/j.matchar.2022.111856.

[34] Zeng, X., Xiong, Y., Liu, Z., Tong, X., Hu, C., Bian, J., Cao, Q., & Cheng, X. (2022). Preparation and characterization of self-lubricating $CaF_2$@$ZrO_2$/YSZ composite coating. *Journal of Thermal Spray Technology*, 31(7), 2126-2135. doi: 10.1007/s11666-022-01424-x.

[35] Zhang, A., Wang, K., Zhang, Y., Ma, G., Yang, W., Zhou, G., Ke, P., & Wang, A. (2024). Towards developing $Ti_2AlC$ coatings with improved oxidation resistance via Nb solid solution. *Journal of Alloys and Compounds*, 1002, article number 175524. doi: 10.1016/j.jallcom.2024.175524.

[36] Zhou, S., Xiang, H., Fang, C., Xu, W., Sun, K., & Zhou, Y. (2026). Ultrasonic-assisted hot-press sintering of Cu-$Ti_3AlC_2$ composites. *Npj Advanced Manufacturing*, 3(1), article number 7. doi: 10.1038/s44334-026-00067-y.

[37] Zhou, Y., Wang, Z., Zhao, J., & Jiang, F. (2023). Effect of ultrasonic amplitude on interfacial characteristics and mechanical properties of Ti/Al laminated metal composites fabricated by ultrasonic additive manufacturing. *Additive Manufacturing*, 74, article number 103725. doi: 10.1016/j.addma.2023.103725.

# Еволюція мікроструктури та зносостійкість фаз MAX на основі титану, легованих елементами X, для застосування у бурінні та видобутку вуглеводнів

**Маріне Сасунцян**

Кандидат технічних наук, доцент
Національний політехнічний університет Вірменії
0009, вул. Терян, 105, м. Єреван, Вірменія
https://orcid.org/0009-0000-6769-114X

**Ніна Саакян**

Кандидат технічних наук
Національний політехнічний університет Вірменії
0009, вул. Терян, 105, м. Єреван, Вірменія
https://orcid.org/0009-0007-6511-7129

**Сероб Айрапетян**

Кандидат технічних наук, науковий співробітник
Національний політехнічний університет Вірменії
0009, вул. Терян, 105, м. Єреван, Вірменія
https://orcid.org/0009-0008-4576-2371

**Сурен Агбалян**

Аспірант
Національний політехнічний університет Вірменії
0009, вул. Терян, 105, м. Єреван, Вірменія
https://orcid.org/0000-0001-9987-8515

**Анотація.** Метою дослідження було з'ясувати, як легування різними елементами групи X впливає на еволюцію мікроструктури сплавів на основі титану з фазою MAX, а також як ці зміни позначаються на твердості, теплофізичних та трибологічних властивостях. Методологія передбачала отримання базової та легованої серій сплавів Ti-Al-C та їх дослідження методами рентгенофазового аналізу, скануючої електронної мікроскопії, енергодисперсійного аналізу, цифрової морфометрії, мікроіндентації, резонансного визначення модуля пружності, дилатометрії, термогравіметричного аналізу, трибологічних випробувань та статистичної обробки даних. У результаті встановлено, що базова серія зберігає домінування $Ti_3AlC_2$ на рівні 87 % і характеризується найбільш впорядкованою пластинчастою мікроструктурою із середнім розміром зерен 8,3 мкм. Легування залізом зменшує частку $Ti_3AlC_2$ до 62 %, збільшує вміст TiC до 28 % і супроводжується появою $Fe_3Al$, подрібненням зерен до 5,7 мкм, порушенням пластинчастої архітектури та розвитком гетерогенного карбідно-інтерметалічного ансамблю. Це забезпечує максимальну мікротвердість 5,1 ГПа, але одночасно призводить до зниження модуля пружності до 191 ГПа, щільності до 4,17 г/см$^3$, електропровідності до $2{,}1\times10^4$ См/м, збільшення коефіцієнта лінійного теплового розширення до $9{,}7\times10^{-6}$ 1/°C, втрати маси за результатами термогравіметричного аналізу до 8,6 % та найгірші трибологічні показники. Легування кремнієм зберігає вміст $Ti_3AlC_2$ на рівні 74 %, супроводжується утворенням $Ti_5Si_3$, сприяє формуванню більш впорядкованої міжзернової структури із середнім розміром зерен 6,9 мкм та забезпечує найбільш збалансований комплекс властивостей: мікротвердість 4,2 ГПа, модуль пружності 214 ГПа, щільність 4,44 г/см$^3$, електрична провідність $3{,}2\times10^4$ См/м, коефіцієнт лінійного теплового розширення $7{,}5\times10^{-6}$ 1/°C, втрата маси за результатами термогравіметричного аналізу – 3,4 %, втрата маси при терті – 3,4 %, знос – 0,28 о.з., а коефіцієнт тертя – 0,47. Практичне значення отриманих результатів полягає у можливості їх використання при розробці та підборі зносостійких MAX-матеріалів на основі титану та покриттів для бурового та нафтогазовидобувного обладнання

**Ключові слова:** розробка карбідів; трибологічні властивості; розмір зерен; модуль пружності; теплопровідність; твердість